23rd ABCM International Congress of Mechanical Engineering
December 6-11, 2015, Rio de Janeiro, RJ, Brazil

NUMERICAL ANALYSIS OF PERFORMANCE DEGRADATION IN MULTISTAGE ELECTRIC SUBMERSIBLE PUMPS

Edgar Minoru Ofuchi
Henrique Stel
Rafael Dunaiski
Thiago Sirino
Rigoberto E. M. Morales
Multiphase Flow Center (NUEM), Postgraduated Program in Mechanical and Materials Engineering (PPGEM), Federal University of Technology – Paraná (UTFPR) – Av. Sete de Setembro, 3165 - Rebouças CEP 80230-901 - Curitiba - PR - Brasil
edgarofuchi@gmail.com; henriqueazevedo@utfpr.edu.br; rafael.dunaiski@gmail.com; thiagosirino@hotmail.com; rmorales@utfpr.edu.br

Abstract. *When handling oils, centrifugal pumps experiment a performance degradation that affects head, flow rate and efficiency. This degradation is related to a decrease of the rotating Reynolds number, which in turn is a function of the impeller speed and fluid viscosity. The effect of the Reynolds number on performance, as well as its relation with other pump dimensionless numbers are still quite unexplored in literature. These issues are addressed in this study through an investigation of the performance degradation in multistage Electric Submersible Pumps (ESPs). Numerical simulations are conducted using two different semi-axial ESPs operating with a wide range of conditions and viscosities. Commercial Computational Fluid Dynamics software, which uses multi-block, transient rotor-stator technique, was used to solve the flow numerically. Dimensional analysis of the flow was adopted to manage the numerical results and correlate performance degradation of both pumps. In addition, dimensionless velocity flow field shows comparison of different operational conditions for constant specific speed. These analyses contribute on the understanding in performance degradation and a useful way to compare the flow behavior in different centrifugal pumps.*

Keywords: *ESP, Performance Degradation, CFD, Reynolds, Specific speed*

1. INTRODUCTION

Artificial lift techniques are used when a given well has its production lowered. They make the well economically viable and provide a longer lifetime of production. One of the most used artificial lift technique is the Electrical Submersible Pump (ESP) system, which is a down-hole system composed of a multistage centrifugal pump. The wide range of flow rates, adaptability to harsh environment and versatility are examples of the benefits of using ESP as an artificial lift technique.

However, pumping viscous oil is generally associated with low Reynolds number flows. This condition leads to a performance degradation respect to the performance expected from the regular operation with water that most of the centrifugal pumps are originally designed for. The degradation occurs mainly due to a significant increase in frictional losses, which eventually decreases the pump head, shifts the best efficiency point down to a lower flow rate and, of course, decreases hydraulic efficiency.

Over the years, many studies have been done to understand how viscosity affects the performance of centrifugal pumps. Ippen (1945) and Stepanoff (1957) studied several types of losses that occur in the centrifugal pumps and the influence of viscosity in these losses. Also, a method to predict performance degradation was proposed by the authors, based on their results. Lately, based on loss analysis, Gülich (2010) presents a methodology to quantify the losses that occurs in the centrifugal pump flow. In addition, the author presents a method to predict performance degradation.

Recently studies involving flow visualization through PIV, LDV or numerical simulation has been used to map the flow inside a centrifugal pump. These works give a better understanding on the flow phenomena. Moreover, they provide detailed information about flow field and interaction of parts of a centrifugal pump, as impeller-diffuser interaction. Examples of such works can be found in Li (2000), Pedersen *et al.* (2003), Feng *et al.* (2010), Sirino (2013) and Stel *et al*. (2014). However, these studies are generally limited to a given centrifugal pump and the performance test in which it is conditioned for.

Dimensional analysis is other way to analyze performance degradation. Solano (2009) and Paternost (2013) conducted experiments to analyze performance degradation, respectively with an ESP and a radial type centrifugal pump. The authors used dimensionless numbers such as specific speed and Reynolds number to express the pumps performances. They also evaluated head degradation using a concept from Stepanoff (1957), who states that performance degradation occurs in such a way that the specific speed remains constant. For both pumps, the authors observed this phenomenon for different rotation speed, fluid viscosity and flow rate. Sirino (2013) and Stel *et al*. (2014) investigated performance degradation on one and three stages (respectively) of an ESP operating with fluids with a range of viscosities. For several conditions of fluid viscosity, impeller rotation speed and flow rate, the authors observed that performance degradation occurs similarly for constant Reynolds number, which indicates a similarity condition for highly viscous fluid flow. This is a useful feature since once can correlate multiple operating conditions for a given pump. How to correlate results for different pumps, however, is still an open matter.

Following the issues stated above, this paper presents a CFD work on the evaluation of performance degradation in two ESPs with three stages as function of dimensionless numbers. The presented analysis provides information about how performance degradation occurs and the behavior of the flow field when the pumps operate with highly viscous fluids.

2. ESP DESCRIPTION

The Reda Schlumberger™ GN7000 and GN5200 540 Series are the ESPs models considered in this study. Both models have semi-axial impellers with seven blades, followed by diffusers with seven vanes. Figure 1-(a) shows a schematic view of the parts of a multistage ESP system. A long cylindrical housing houses the stages, which each stage is composed by an impeller and a diffuser. The shaft provides kinetic energy from the electrical motor to the impeller, where it is converted to an increase in pressure. Figure 1-(b) presents a picture of cut pieces of one stage that shows the position of the shrouds, hubs blade and vane from impeller and diffuser. Figure 1-(c) shows a cross section view of an impeller and a diffuser, which indicates the position of the blades and vanes, the main representative diameters and a position of a midspan surface that is located at the middle distance of the hubs and shrouds of the impeller and the diffuser. Figure 1-(d) shows a schematic representation taken from the midspan surface of a single channel of one stage, where indicates a generic interface, the pressure and suction sides of the blades and vanes, as well as the inlet and outlet blade/vane thicknesses and angles. For the ESPs used in this work, the single channel is equivalent to one seventh of the whole stage and is equal to 360º/7 = 51.43º.

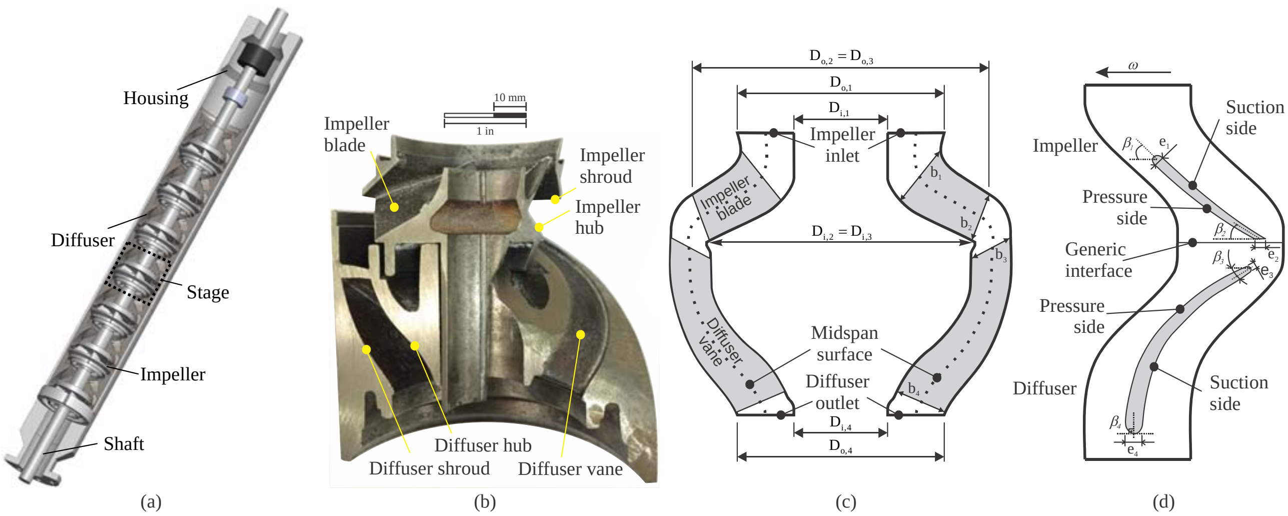

Figure 1. Schematic view of an ESP system (a), cut pieces (b), cross-section view (c) and midspan surface view (d).

The main dimensions and specifications of the impeller and diffuser previously indicated in Figs. 1-(c) and 1-(d) are shown in Tab. 1, where the indices 1, 2, 3 and 4 refer to impeller inlet, impeller outlet, diffuser inlet and diffuser outlet, respectively, while indices *i* and *o* correspond to inner and outer diameters of each cross-section area. Z is the number of blades (impeller) or vanes (diffuser), while *b*, *e* and β denote their height, thickness and angle, respectively. The nominal shaft and housing diameters are 25.4 mm (1 inch) and 168.3 mm (6.625 inches) for the ESPs considered.

From the manufacture's catalog, when operating with water at a 3500rpm rotation speed, the GN7000 ESP is designed to deliver Q_{des} = 1.360x10^{-2} m³/s and H_{des} = 9.6 m per stage, while the GN5200 model gives Q_{des} = 1.006x10^{-2} m³/s and H_{des} = 8.6 m per stage, all at the best efficiency point. The specific speed of the GN7000 and GN5200 ESPs at these conditions are respectively $n_q = n_{des}\sqrt{Q_{des}} / H_{des}^{0.75} = 74.6$ and $n_q = n_{des}\sqrt{Q_{des}} / H_{des}^{0.75} = 69.7$, where n_{des} is in rpm, Q_{des} in m³/s and H_{des} in m.

Table 1. Main dimensions and specifications of the impeller and the diffuser of the ESPs GN7000 and GN5200 ESPs.

	GN7000		GN5200	
Description	Impeller	Diffuser	Impeller	Diffuser
Number of blades/vanes	$Z = 7$	$Z = 7$	$Z = 7$	$Z = 7$
Inlet inner diameter	$D_{i,1} = 29.8$ mm	$D_{i,3} = 83.1$ mm	$D_{i,1} = 30.2$ mm	$D_{i,3} = 79.7$ mm
Outlet inner diameter	$D_{i,2} = 83.1$ mm	$D_{i,4} = 29.8$ mm	$D_{i,2} = 79.7$ mm	$D_{i,4} = 30.2$ mm
Inlet outer diameter	$D_{o,1} = 65.7$ mm	$D_{o,3} = 93.7$ mm	$D_{o,1} = 65.3$ mm	$D_{o,3} = 93.3$ mm
Outlet outer diameter	$D_{o,2} = 93.7$ mm	$D_{o,4} = 65.7$ mm	$D_{o,2} = 93.3$ mm	$D_{o,4} = 65.3$ mm
Inlet blade height	$b_1 = 20.7$ mm	$b_3 = 14.3$ mm	$b_1 = 22.6$ mm	$b_3 = 14.5$ mm
Outlet blade height	$b_2 = 15.9$ mm	$b_4 = 16.7$ mm	$b_2 = 15.4$ mm	$b_4 = 17.8$ mm
Inlet blade thickness	$e_1 = 2.4$ mm	$e_3 = 3.1$ mm	$e_1 = 1.8$ mm	$e_3 = 3.4$ mm
Outlet blade thickness	$e_2 = 3.0$ mm	$e_4 = 4.5$ mm	$e_2 = 2$ mm	$e_4 = 4.3$ mm
Inlet blade angle	$\beta_1 = 27^o$	$\beta_3 = 29^o$	$\beta_1 = 16^o$	$\beta_3 = 31^o$
Outlet blade angle	$\beta_2 = 42^o$	$\beta_4 = 90^o$	$\beta_2 = 35^o$	$\beta_4 = 90^o$

3. NUMERICAL APROACH

ANSYS-CFX™ is the software used to solve numerically the present problem. Turbulence is modeled using an eddy-viscosity based model, the resultant set of equations being called commonly as the Unsteady Reynolds-Averaged Navier-Stokes (U-RANS) equations. The software uses an element-based finite-volume method to discretize equations in the spatial domain. In addition, a High Resolution scheme and the second order backward Euler are used for the advection and time discretization, respectively (ANSYS, 2014).

The Shear Stress Transport (SST) turbulence model with automatic wall treatment was used (ANSYS, 2014). For cases when the pump operates with highly viscous fluids, a laminar flow regime was assumed. The estimation of such condition was done using a Reynolds number, $\mathrm{Re}_{D_h} = \rho V D_h / \mu$, based on the hydraulic diameter of the channels, D_h, where V is the average velocity through the hydraulic channels cross-section areas. The critical Reynolds number value assumed to judge the flow regime inside the centrifugal pump was $\mathrm{Re}_{D_h} = 2000$.

Figure 2-(a) shows a simplified scheme of the numerical domain, where three stages of each ESP are considered. Two pipes (intake and discharge) are positioned at the last diffuser outlet and the first impeller inlet to minimize any numerical instability related to boundary conditions. A specified flow rate is imposed at the outlet of the discharge pipe for each simulation, as well as a reference pressure at the inlet intake pipe, $P_{ref} = 0$ [Pa]. A medium turbulence intensity ($\mu_t / \mu = 10$) is assumed at the inlet. The pipes and diffusers walls are no-slip and smooth, while in the impellers they move with constant rotation speed. The ESPs have seven hydraulic channels, but this periodicity allows simulating only a single channel using a rotational-periodic boundary condition, which greatly reduces the computational cost of the simulations.

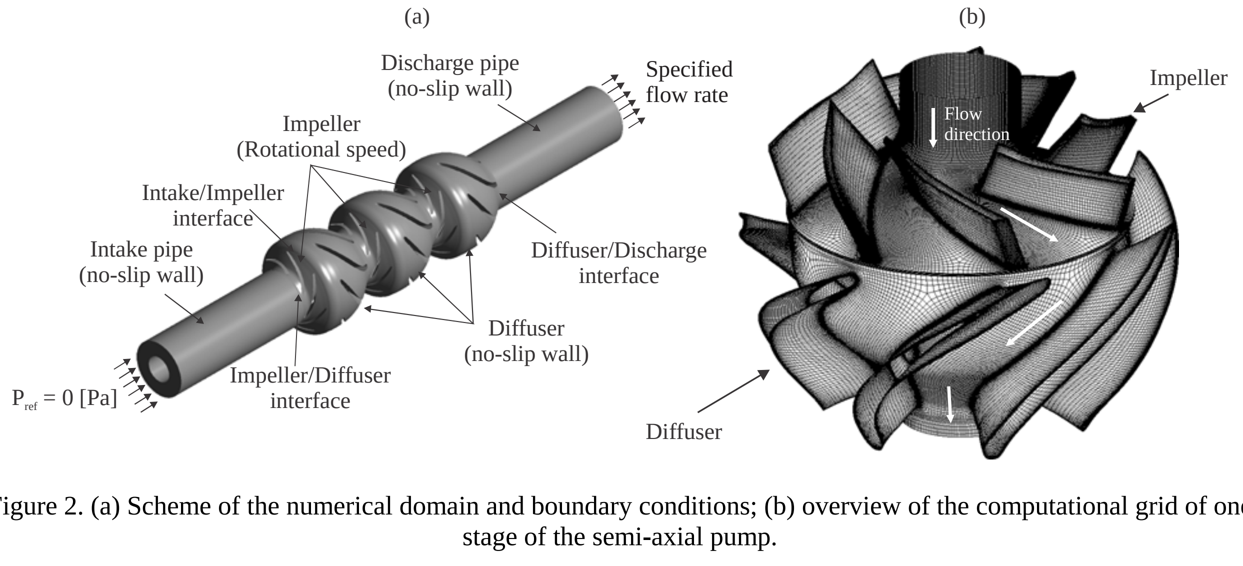

Figure 2. (a) Scheme of the numerical domain and boundary conditions; (b) overview of the computational grid of one stage of the semi-axial pump.

For turbomachinery flow simulations, ANSYS CFX^{TM} uses a multi-block technique, which considers each component of the pump as a separated subdomain. The interfaces that connect each domain are calculated by the Generic Grid Interface (GGI) and the Multiple Frame of Reference (MRF) algorithms (ANSYS, 2014). These algorithms accounts for static (Diffuser/Discharge) and moving (Impeller/Diffuser) interfaces. For the moving interface, the algorithms apply a tangential displacement to the rotating part at each time step before transferring the information across the interface.

The numerical structured grid and a rough indication of the flow path are shown in Fig 2-(b). The hexahedral elements are refined near the walls, especially in the blade and vane edges. The impellers of the GN7000 and GN5200 ESPs have 603,000 and 496,000 elements, the diffusers have 535,000 and 554,000 elements, while in total is 3,500,000 and 3,300,000, respectively. A mesh sensitivity test was conducted with a mesh two times bigger than the used one. This test showed that the differences for head and efficiency are negligible when the grid is refined more than the presented mesh.

A steady-state simulation is used before each transient simulation to provide an average flow field as initial condition. This procedure allows less numbers of time steps required for a statistically converged transient solution. A total of 420 time steps are used in almost all simulations, which is equivalent to five complete revolutions.

4. RESULTS AND DISCUSSION

4.1 Comparison with experiments and catalog data

Numerical results for head are compared with experimental results from Amaral(2007) and catalog data. Amaral (2007) tested the GN7000 ESP with three stages for several rotation speed and fluid viscosities. Details of his work are found in Amaral (2007) and Amaral et al. (2009).

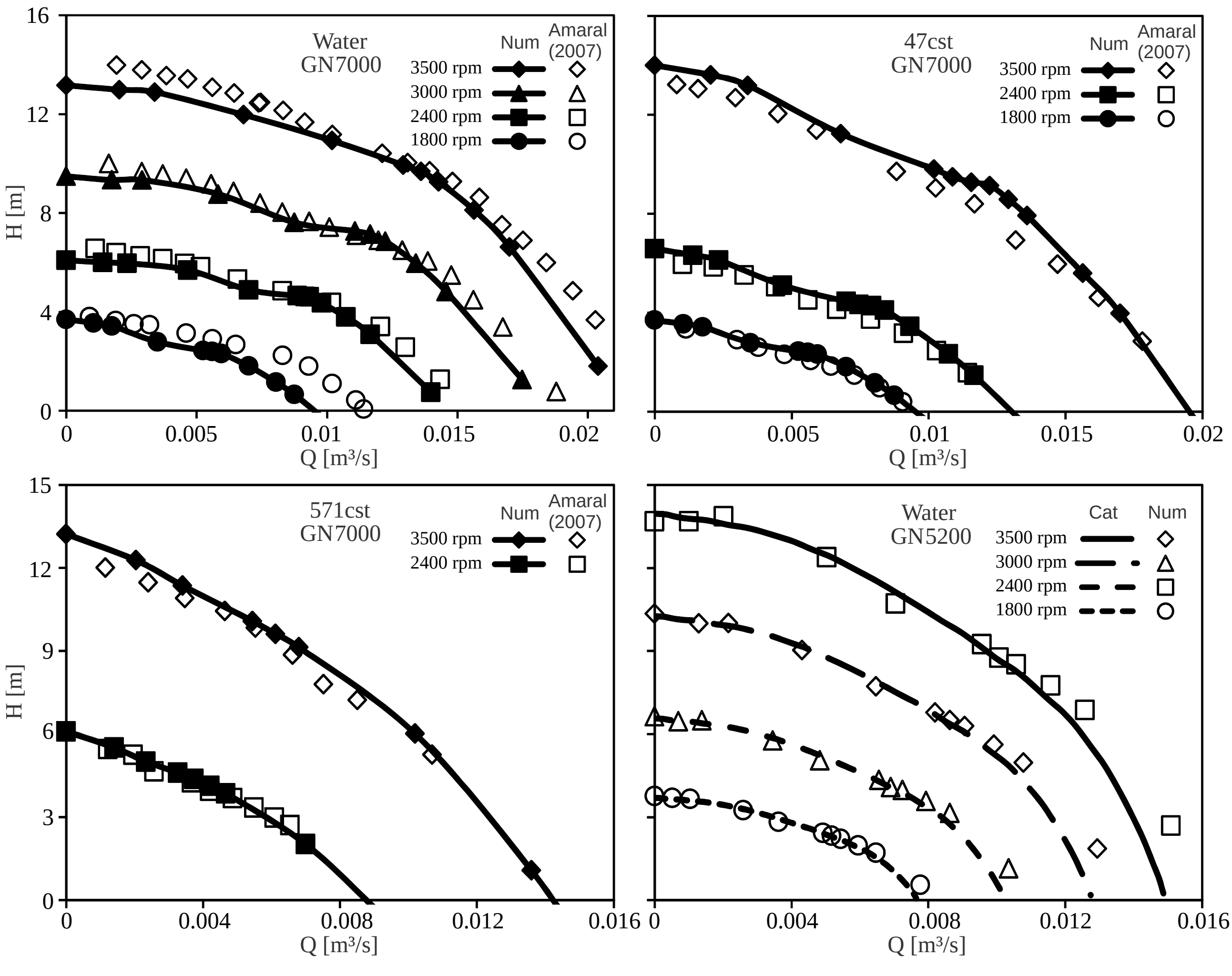

Figure 3. Comparison of numerical and experimental (Amaral, 2007) head values for the GN7000 ESP operating with different fluid viscosities and rotation speeds, as well as a comparison of numerical and catalog data for operation with water at different rotation speeds for the GN5200 ESP.

Figure 3 shows the comparison between numerical, experimental and catalog head curves as function of flow rate for different rotation speed and fluid viscosities. For the GN7000 ESP, the numerical curves were compared to the experimental data from Amaral (2007) for three fluid viscosities and several rotating speeds. One can observe that the numerical data agree well with the experiments. In addition, the agreement increases for higher viscosities. The coefficient of determination, R^2, is used to evaluate the differences between numerical results with the other sources. For the GN7000 model, the coefficients of determination for all curves are within 0.96 and 0.99. For the ESP GN5200 model, no experimental data was available in literature, so catalog data was used. The comparison with the manufacturer's curves showed a good agreement, the coefficient of determination being within 0.97 and 0.99.

4.2 Performance degradation

A dimensionless analysis is conducted to obtain dimensionless groups to evaluate performance degradation in the centrifugal pumps. The Buckingham's Pi method is used to obtain the following dimensionless groups:

$$\Psi = \frac{gH}{\Omega^2 D_2^2},\ \Phi = \frac{Q}{\Omega D_2^3},\ \mathrm{Re}_\omega = \frac{\Omega D_2^2}{\nu}\ \text{and}\ \omega_s = \Omega\frac{Q^{1/2}}{\left(gH\right)^{3/4}} \tag{1}$$

where Ψ, Φ, Re_ω and ω_s are, respectively, head coefficient, flow coefficient, rotational Reynolds number and specific speed. In fact, the former is a combination of the head and flow coefficients. Constant g is the gravitational acceleration in [m/s²], Ω is the angular speed in [rad/s], D_2 is the impeller outlet diameter in [m], Q is the flow rate in [m³/s], H is the head in [m] and ν is the kinematic viscosity in [m²/s].

Solano (2009) and Sirino (2013) showed that it is convenient to use a normalized form of the dimensionless groups. The normalization was made using the variables at the design condition (subscript "*des*") which is equivalent to the best efficiency point in the catalog data, resulting in the following form:

$$\Psi_n = \frac{H}{H_{des}}\left(\frac{\omega_{des}}{\omega}\right)^2,\ \Phi_n = \frac{Q}{Q_{des}}\frac{\omega_{des}}{\omega},\ \mathrm{Re}_n = \frac{\Omega}{\Omega_{des}}\frac{\nu_{des}}{\nu}\ \text{and}\ \omega_n = \frac{\omega_s}{\omega_{s,des}} \tag{2}$$

where Ψ_n, Φ_n, Re_n and ω_n are normalized head coefficient, normalized flow coefficient, normalized rotational Reynolds number and normalized specific speed, respectively.

Stepanoff (1957) stated that for viscous fluid operation, head and flow rate degrade in such a manner that specific speed remains constant at the best efficiency point (BEP). Using this idea, Solano (2009) evaluated performance degradation for three values of specific speed in the same pump, which corresponded to points at the BEP, at a part load condition and at an overload condition. The author observed that for all specific speeds, performance degradation occurred for a constant specific speed.

A similar analysis is presented in this work, but using the normalized specific speed, ω_n, instead. Figure 4-(a) shows the degradation of normalized head coefficient as function of the normalized flow coefficient, for three values of normalized specific speed. Numerical results from both the GN5200 and GN7000 ESPs are plotted. Experimental data for a radial type centrifugal pump, Imbil ITAP 65/330, from Amaral (2007) is also presented to compare with the semi-axial type ESPs. The radial centrifugal pump ITAP is a two stage centrifugal pump with radial impellers with different diameters, a vaned diffuser followed by a vaned return channel that connects the stages and a volute.

One observes from Fig. 4-(a) that the normalized head and flow coefficients degrade with a decrease in the normalized rotational Reynolds number. Moreover, results from all pumps follow the same curve of constant normalized specific speed, which indicates that the normalization procedure is a useful tool in this case. A design water curve is also shown in Fig. 4-(a) to explain that each degraded point has its equivalent "degraded" condition in the water design curve, for a constant normalized specific speed that intercepts the water curve.

Based on his observations that performance degradation occurs for constant specific speed, Solano (2009) proposed the use of correction factors, which is a normalization related to the design water curve at a given normalized specific speed, given by:

$$C_H = \left.\frac{\Psi_n}{\Psi_{n,w}}\right|_{\omega_n} = \left.\frac{H}{H_w}\left(\frac{n_w}{n}\right)^2\right|_{\omega_n},\ C_Q = \left.\frac{\Phi_n}{\Phi_{n,w}}\right|_{\omega_n} = \left.\frac{Q}{Q_w}\frac{n_w}{n}\right|_{\omega_n} \tag{3}$$

where C_H and C_Q are the head and flow correction factors, while the subscript w represents the condition for water at the catalog rotational speed.

Stepanoff (1957) showed that for a constant specific speed and rotation speed, there is a correlation between head and flow correction factors:

$$\frac{\Omega\sqrt{Q_v}}{\left(gH_v\right)^{3/4}} = \frac{\Omega\sqrt{Q_{des}}}{\left(gH_{des}\right)^{3/4}} \rightarrow \left(\frac{Q_v}{Q_{des}}\right)^{1/2} = \left(\frac{H_v}{H_{des}}\right)^{3/4} \rightarrow F_Q = F_H^{1/2} \tag{4}$$

where F_Q and F_H are the flow and head correction factors used by Stepanoff (1957), and the subscript v is the value for viscous operation. This relation was found to also hold when using C_Q and C_H from Eq. (3):

$$C_Q = C_H^{1.5} \tag{5}$$

Figure 4-(b) shows the numerical and experimental data presented in Fig. 4-(a) after the modification of the normalized dimensionless groups to correction factors. Despite the difference in the formulation of the correction factors, one can observe that all data from the three centrifugal pumps collapse well on the correlation proposed by Stepanoff (1957).

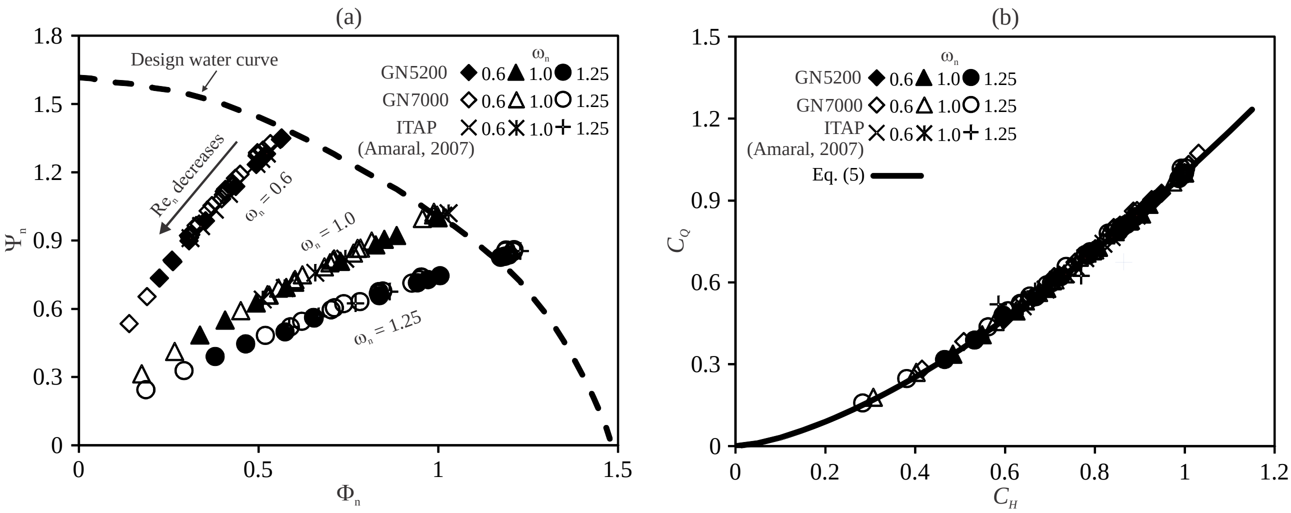

Figure 4. (a) Normalized head coefficient versus normalized flow coefficient for three different normalized specific speeds, using numerical results from two semi-axial ESPs and data from Amaral (2007) for the radial centrifugal pump; (b) flow correction factor as a function of the head correction factor.

Performance degradation has shown that a relation exists between head and flow rate degradation with an increase in viscosity. For this reason, an analysis of the flow field has been conducted to verify if there is a relationship between velocity flow field and viscosity for a constant normalized specific speed.

Figure 5 shows the dimensionless velocity flow field at the midspan surface for constant normalized specific speed, ω_n=1.0, at three different operational conditions for the second stage of the three stage ESPs. A dimensionless velocity was used, which is the ratio between the transient-average velocity, $\overline{V}$, and the tangential velocity U_2. Both velocities are expressed as:

$$\overline{V} = \frac{1}{T}\int_t^{t+T} V\left(t\right)dt \qquad U_2 = \frac{\Omega D_2}{2} \tag{6}$$

where T is the total time of simulation in [s], $V(t)$ is the instantaneous velocity in [m/s], D_2 is the impeller outlet diameter in [m] and Ω is the angular speed in [rad/s].

One can observe in Fig. 5 that comparing the dimensionless velocity flow fields, for different conditions at a constant normalized specific speed, does not show a clear hydrodynamic similarity between them. However, note that there are some similar flow characteristics between the flow in the ESPs. For example, a flow separation structure found near the diffuser outlet for 1cst. In addition a jet-wake structure is found at the impeller blade outlet for both pumps. With the increase in viscosity, the normalized flow coefficient diminishes and for the 47 and 48cst fluids the flow separation found near the diffuser outlet increases, and a flow recirculation is generated near the impeller trailing edge for the GN5200 model. For a higher viscosity, 571 and 580cst, the recirculations disappeares due to the highly viscous influence on the flow structure. Also an increase in the velocity boundary layer can be seen near the diffuser and impeller walls.

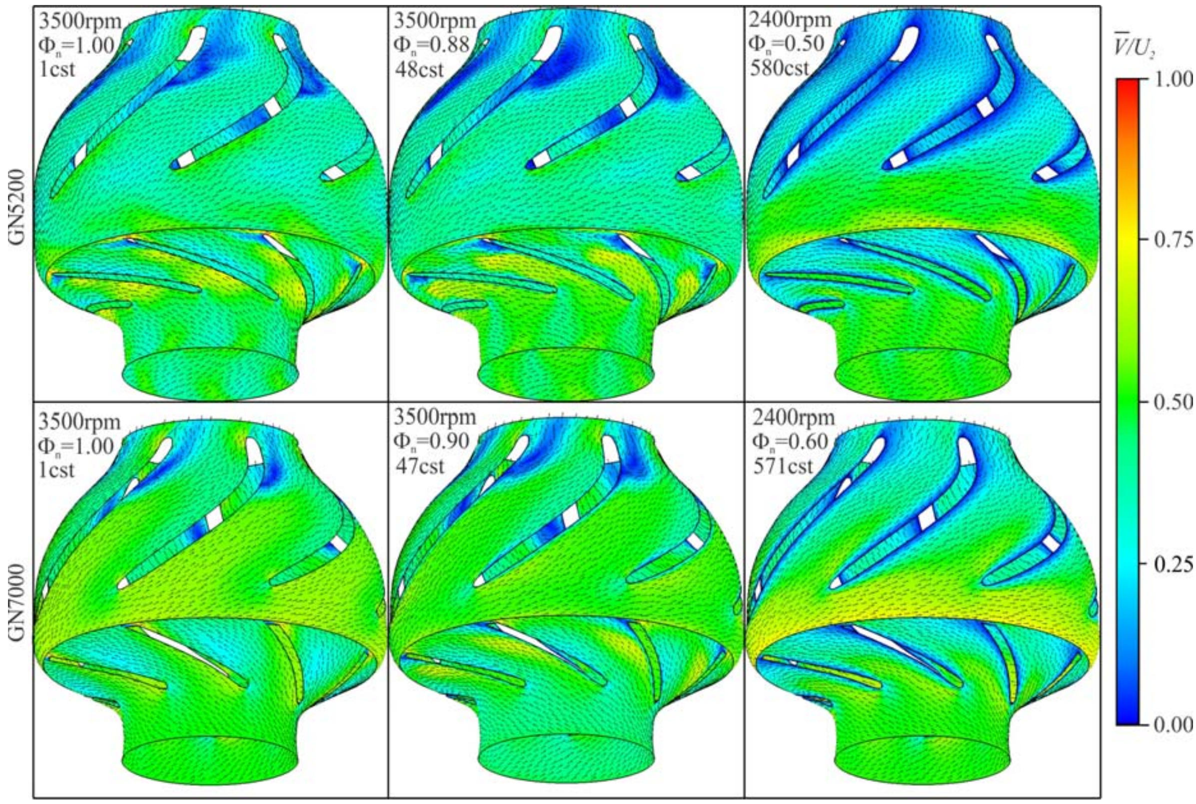

Figure 5. Dimensionless velocity flow field at the midspan surface for constant normalized specific speed, ω_n=1.0, for GN5200 and GN7000 at different operational conditions for the second stage of the three stage ESPs.

A strong relashionship between the dimensionless velocity flow field and performance degradation for a constant normalized specific speed was not found. However, analyzing the flow field for constant rotational Reynolds number shows equivalent flow fields, as presented in Fig. 6. This figure shows the instantaneous dimensionless velocity flow fields for both the GN5200 and GN7000 ESPs at the second stage impeller, for different operational conditions but same rotation Reynolds number. For a given pump, one can observe that the velocity flow field is identical in spite of the difference of the operational conditions, which indicates a hydrodynamic similarity condition. Even the flow separation are located at the same position, as one can clearly observe. However, differences in the flow field between the ESPs are expected due to the geometrical differences.

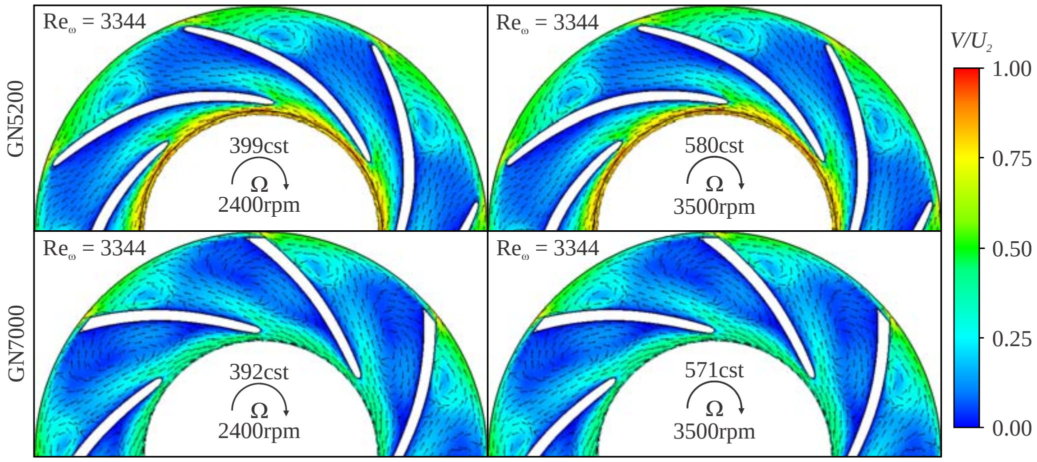

Figure 6. Instantaneous velocity flow field for both pumps at the second impeller for different operational conditions and same rotational Reynolds number.

5. CONCLUSIONS

A performance degradation analysis was conducted using CFD to simulate the flow inside two ESPs with three stages. Numerical head values was compared with experimental and catalog data. This validation showed good agreement for operation with several fluid viscosities, impeller speeds and a large range of flow rates, for both pumps.

Dimensional analysis was conducted and proved to be a good way to evaluate performance degradation. Using the proper dimensionless groups, different centrifugal pumps presented the same behaviour of head and flow rate degradation. In addition, a known expression from literature was used to correlate flow and head correction factors, and agreed well with the numerical results and experimental data.

An investigation about the behaviour of the velocity flow field was also presented. However a clear hydrodynamic similarity between the flow field and the increase in viscosity for constant normalized specific speed was not found. Still, when comparing two different operational conditions but same rotational Reynolds number, an identical flow field was observed, which indicates a hydrodynamic similarity condition.

The good agreement between performance degradation for different centrifugal pumps shows that the present anlaysis could be extended to other pumps. Moreover, with a proper relation between one of the correction factors, a procedure to predic perfomance degradation can be proposed.

ACKNOLOGMENTS

The authors acknowledge the financial support from CAPES foundation, ANP and FINEP through the Human Resources Program to oil, the gas segment PRH-ANP (PRH 10 - UTFPR) and from TE / CENPES / PETROBRAS.

REFERENCES

Amaral, G., 2007, “Modelagem do Escoamento Monofásico em Bomba Centrífuga Submersa Operando com Fluidos Viscosos (Modeling of the Single-Phase Flow in an Electrical Submersible Pump Operating with Viscous Fluids)”, MS thesis (in Portuguese), State University of Campinas, Campinas, Brazil.

Amaral, G., Estevam, V. and França, F. A., 2009, “On the Influence of Viscosity on ESP Performance,” *SPE Production & Operations*, 24(2), pp. 303-310.

Pedersen, N., Larsen, P. S. and Jacobsen C.B., 2013, “Flow in a Centrifugal Pump Impeller at Design and Off-Design Conditions – Part I: Particle Image Velocimetry (PIV) and Laser Doppler Velocimetry (LDV) Measurements,” *Journal of Fluids Engineering*, pp. 61-72.

ANSYS, 2014, "ANSYS - Solver Theory Guide", ANSYS Inc., Canonsburg, PA.

Feng. J., Benra F. K. and Dohmen H. J., 2010, “Unsteady flow investigation in rotor-stator interface of a radial diffuser pump”, *Forsch Ingenieurwes*, pp 233-242.

Gülich, J. F., 2010, *Centrifugal Pumps*, Springer, Berlin 2nd edition.

Ippen, A. T., 1945, “The Influence of Viscosity on Centrifugal Pump Performance,” Issue 199 of *Fritz Engineering Laboratory report*, ASME Paper No. A-45-57.

Li. W.G., 2000, “Effects of viscosity of fluids on centrifugal pump performance and flow pattern in the impeller” *International Journal of Heat and Fluid Flow*, pp. 207-212.

Paternost. G. M., 2013, “Estudo Experimental Sobre Bomba Centrífuga Operando com Fluido Viscoso e Escoamento Bifásico Gás-Líquido (Experimental study about the flow in a centrifugal pump operating with viscous fluid and two-phase gas-liquid flow), MS thesis (in Portuguese), State University of Campinas, Campinas, Brazil.

Sirino, T., 2013, “Estudo Numérico da Influência da Viscosidade no Desempenho de uma Bomba Centrífuga Submersa (Numerical Study of the influence of viscosity on performance of an Electrical Submersible Pump)”, MS thesis (in Portuguese), Federal University of Technology – Paraná, Curitiba, Brazil.

Solano, E. A., 2009, “Viscous Effects on the Performance of Electro Submersible Pumps (ESP’s),” MS thesis, The University of Tulsa, Tulsa, OK.

Stel, H.; Sirino, T.; Prohmann, P. R.; Ponce, F.; Vicent, S. C.; Morales, R. E. M, 2014, “CFD investigation of the effect of viscosity on a three-stage electric submersible pump”. In: *ASME Fluids Engineering Division Summer Meeting – FEDSM2014*, Chicago, Illinois, EUA.

Stepanoff, A. J., 1957, *Centrifugal and Axial Flow Pumps: Theory, Design and Application*, John Wiley & Sons, New York, 2nd edition.